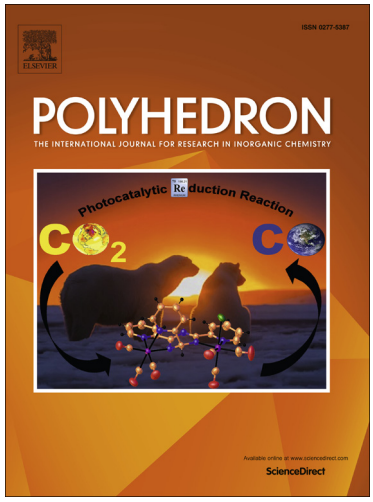

Synthesis, physicochemical properties and *in-vitro* catalytic activity of a dinuclear nickel(II) complex with a N_5O-hexadentate ligand: A functional model for phosphohydrolases

Fernando R. Xavier, Ademir Neves

PII: S0277-5387(16)00098-X
DOI: http://dx.doi.org/10.1016/j.poly.2016.02.013
Reference: POLY 11828

To appear in: *Polyhedron*

Received Date: 16 September 2015
Accepted Date: 8 February 2016

Please cite this article as: F.R. Xavier, A. Neves, Synthesis, physicochemical properties and *in-vitro* catalytic activity of a dinuclear nickel(II) complex with a N_5O-hexadentate ligand: A functional model for phosphohydrolases, *Polyhedron* (2016), doi: http://dx.doi.org/10.1016/j.poly.2016.02.013

Synthesis, physicochemical properties and *in-vitro* catalytic activity of a dinuclear nickel(II) complex with a N_5O-hexadentate ligand: A functional model for phosphohydrolases

by **Fernando R. Xavier**[a]* and **Ademir Neves**[b]

[a]Departamento de Química, Universidade do Estado de Santa Catarina, Joinville – SC, Brazil. CEP 89219-710; [b]Departamento de Química, Universidade Federal de Santa Catarina, Florianópolis – SC, Brazil. CEP 88040-900; *Corresponding author: fernando.xavier@udesc.br

Abstract

The development of artificial nucleases has been stimulated by the realization that hydrolytically active metal complexes may potentially find utility as robust versatile replacements for restriction enzymes in molecular biology research and as nucleic acid-targeting therapeutics. In this regard, a novel unsymmetrical dinucleating ligand **HL** (where L is the 2-[(4,7-diisopropyl-1,4,7-triazonan-1-yl)methyl]-4-methyl-6-[(pyridin-2-ylmethylamino)methyl]phenolate moiety) with an N_5O-donnor set was synthesized and characterized by IR and ^{1}H-NMR spectroscopy. The reaction of HL with nickel(II) perchlorate led to the formation of a μ-phenoxo-bridged dinuclear Ni(II) complex, $[Ni_2(L)(\mu\text{-}OAc)_2]BPh_4 \bullet H_2O$ (**1**). Physicochemical measurements (molar conductometry, IR and UV-visible spectroscopy and electrochemistry) were performed for **1** and

these properties are compared with those presented by similar compounds in the literature. ESI-MS measurements in positive and negative modes confirmed the complex composition as well as the presence of tetraphenylborate counterions, based on their mass and isotopic distribution patterns. Potentiometric titration studies of **1** were carried out (CH_3CN/H_2O 50% v/v) and we probed its acid/base properties, which are crucial to gaining an understanding of the phosphodiester catalytic cleavage mechanism. Finally, the ability of **1** to mimic the functional role of the dinuclear metalloenzymes was evaluated through studies on its reactivity toward the model-substrate bis(2,4-dinitrophenyl)phosphate (2,4-bdnpp). When compared with similar previously described compounds, complex **1** helped to probe the influence of the aromatic/aliphatic *N*-donor moieties, such as macrocyclic rings, pyridine and imidazole, through their catalytic efficiency parameter ($E / L\ mol^{-1}\ s^{-1}$).

1. Introduction

Phosphate esters are omnipresent in the area of biology, where they fulfil a number of key roles. They are found in the hydrophilic "head" group of phospholipids (the major component of cell membranes) and in many small molecules that play a role in metabolism, such as ATP, coenzyme A and cAMP.[1] However, probably the most notable biological structures that employ phosphate esters moieties are deoxyribonucleic acid (DNA) and ribonucleic acid (RNA). Chemically, these biopolymers are comprised of ribonucleotides or deoxyribonucleotides in RNA and DNA, respectively, and the monomers are connected through their 3',5'-phophodiester bonds [1] .

The uncatalyzed hydrolysis of phosphodiesters is favored thermodynamically but in terms of kinetics it is exceedingly slow, making them particularly robust in their structural roles in biology. In particularly, in DNA these bonds have an estimated half-life of 30,000,000 years (pH 6.8, 25 ◦C), calculated from the rate of hydrolysis of dineopentyl phosphate measured under these conditions (7×10^{-16} s^{-1}) [2] . The nucleophilic cleavage of phosphodiester bonds entails the attack of a nucleophile on the phosphorus atom of a phosphodiester moiety, via a pentacoordinate, trigonal bipyramidal, transition state in which the attacking nucleophile and departing alkoxide generally occupy the apical positions [3] .

In this context, the search for low molecular weight catalysts for phosphodiester cleavage has attracted much interest among scientists, since these compounds may help to elucidate several issues such as the cleavage mechanism, the role of metals in these biological systems, and the design of more effective synthetic hydrolases [4] [5] . Since many hydrolytic enzymes contain two metal centers at their active site, which operate in a cooperative fashion to cleave their substrates, it is not surprising that in recent decades there has been intense interest in the development of binuclear metal complexes as a route to generating more active synthetic cleavage agents [6] .

In particularly, dinucleating ligands containing pyridyl pendant arms or *N*-donor macrocyclic motifs are among the most studied compounds, where their metal complexes have shown prominent catalytic activity [4] [6] . However, given that dinuclear metalloenzymes usually present an unsymmetrical feature around

the metal centers in their active sites, there is a significantly smaller number of catalysts with unsymmetrical bioinspired ligands.

In this regard, for several years our group has been engaged in obtaining symmetrical and unsymmetrical homodinuclear $Zn^{II}Zn^{II}$, [7] $Cu^{II}Cu^{II}$, [8] -[12] $Ni^{II}Ni^{II}$, [13] -[15] $Fe^{III}Fe^{III/II}$, [16] -[18] $Mn^{III}Mn^{II}$, [19] -[21] and heterodinuclear $Fe^{III}M^{II}$ (M^{II} = Mn, Co, Ni, Cu, Zn) complexes which are able to hydrolyze the model substrate 2,4-bdnpp and hydrolytically cleave DNA [5] [22] .

Particularly in the bioinorganic field, the macrocycle 1,4,7-triazacyclononane (*tacn*) and a diversity of multidentate functionalized derivatives have proven to be an outstanding approach to ligand design, mostly due to their *facial* coordination mode [4] [6] [8] [23] . Although some unsymmetrical ligands capable of providing distinct chemical environments to yield mixed-valence compounds [5] [6] [22] are described in the literature, to date there are only a few examples of unsymmetrical homodinuclear complexes with a *tacn*-containing dinucleating archetype. One good example is the ligand L^{N3N4} described by Costas and coworkers where *tacn* and pyridyl coordinating units are present [24] .

In this paper, we describe the synthesis and characterization of a new unsymmetrical *tacn*-containing dinucleating ligand 2-[(4,7-diisopropyl-1,4,7-triazonan-1-yl)methyl]-4-methyl-6-{[(pyridin-2-ylmethyl)amino]methyl}phenol (**HL**) and its dinickel(II) complex (**1**) (Chart 1). It is noteworthy that the possibility of providing a free coordination site on one of the nickel centers allows the coordination of an extra labile ligand (e.g., OH_2 groups) which can be easily substituted by the substrate during the catalytic process.

<< Please add Chart 1 here, as a single-column picture >>

Chart 1. Chemical structures of the ligand HL (left) and its nickel(II) cation complex **1** (right).

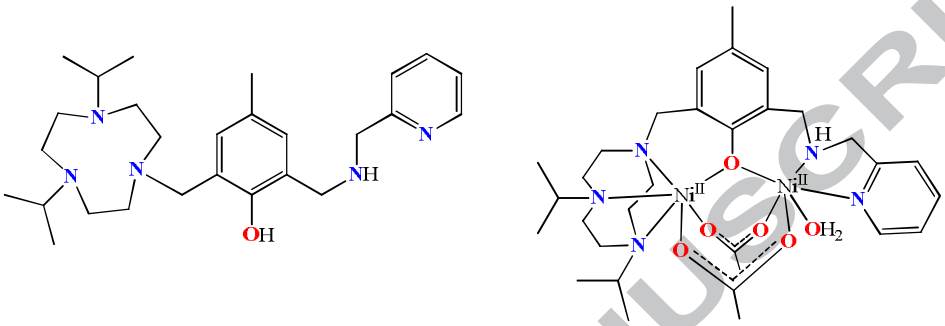

2. Experimental Section

2.1 Chemicals and instrumentation

All starting materials were purchased from Aldrich, Acros or Merck and used as received unless otherwise stated. 2-(aminomethyl)pyridine was distilled under reduced pressure, tetrabutylammonium hexafluorophosphate was double recrystallized from hot ethanol.

Elemental analysis (C, H and N) was performed on a Perkin-Elmer 2400 analyzer equipped with an AD-4 autobalance setup.

Infrared spectra were collected on a Perkin-Elmer FTIR-2000 spectrophotometer using KBr pellets in the range of 4000-500 cm^{-1}. The data were plotted as transmittance (%) as a function of the wavenumber (cm^{-1}).

^{1}H-NMR spectroscopy was carried out with a Varian FT-NMR 400 MHz system, using $CDCl_3$ as the solvent, at 25 °C. Chemical shifts were referenced to tetramethylsilane (TMS, $\delta = 0.000$ ppm).

The molar conductivity for complex **1** was evaluated in a Schott-Geräte CG 853 conductivimeter (previously calibrated with an aqueous 1.00×10^{-2} M KCl solution; Λ_M = 1408 μS [25]) at room temperature using a 1.00×10^{-3} M spectroscopic grade acetonitrile solution.

The electrospray ionization-mass spectrometry (ESI-MS) of **1**, dissolved in an ultrapure acetonitrile solution (500 nM), was performed on an amaZon X Ion Trap MS instrument (Bruker Daltonics) with an ion spray source using electrospray ionization in positive and negative-ion modes. The ion source condition was an ion spray voltage of 4.5 kV. Nitrogen was used as the nebulizing gas (20 psi) and curtain gas (10 psi), and samples were directly infused into the mass spectrometer at a flow rate of 180 μL h^{-1}. The m/z scan range was 150 to 2000 Da. The simulated spectrum was calculated using the mMass software [26] [27] .

UV–visible spectra were obtained at room temperature using a Perkin Elmer Lambda 19 spectrophotometer operating in the range of 300–1000 nm with quartz cells. Values of ε are given in M^{-1} cm^{-1}. The UV-Vis spectrum of **1** was recorded in acetonitrile (spectroscopic grade) solution.

The electrochemical behavior of **1** was investigated with a Bioanalytical Systems Inc (BASi) potentiostat/gavanostat. Square-wave voltammograms were obtained at room temperature in acetonitrile solutions containing 0.1 M of *n*-Bu_4NPF_6 as the supporting electrolyte under argon atmosphere. The electrochemical cell employed was comprised of three electrodes: gold (working), platinum wire (auxiliary) and Ag/Ag^+ (reference). The ferrocene/ferrocinium

redox couple Fc/Fc^+ (E^0 = 400 mV *vs* NHE) [28] was used as the internal standard.

The protonation constants for complex **1** were investigated with a Corning 350 pH meter fitted with a glass-combined electrode (Ag/AgCl) calibrated to read –log $[H^+]$ directly, designated as pH. The experiment temperature was stabilized at 25.00 ± 0.05ºC. Doubly distilled water in the presence of $KMnO_4$ was used to prepare CH_3CN/H_2O (50:50 v/v) solutions. The electrode was calibrated using the data obtained from a titration of a known volume of a standard 1.00×10^{-2} M HCl solution with a standard 0.100 M KOH solution. The ionic strength was kept constant at 0.1 M by addition of KCl, and the solutions, containing 5×10^{-2} mmol of complex, were titrated with 0.100 M standard CO_2-free KOH. Experiments were performed in 50.00 mL of a CH_3CN/H_2O (50:50 v/v) solvent system, purged with argon cleaned using two bubbling towers with 0.1 M KOH solutions. The titration process was initiated around pH 3.0 by the addition of HCl. The experiments were run at least in triplicate and were all analyzed using the BEST7 [29] program. The species diagrams were obtained with SPE and SPEPLOT programs [29] .

2.2 Kinetic assays

The catalytic activity of **1** towards the activated phosphodiester 2,4-bis(dinitrophenyl)phosphate (2,4-bdnpp) [30] was evaluated spectrophotometrically on a Varian Cary50 Bio spectrophotometer, at 400 nm based on the appearance of the 2,4-dinitrophenylphenolate ion at 25 °C. The effect of pH on the hydrolytic cleavage of 2,4-bdnpp was monitored in the pH range

from 4.0 to 10.5. Reactions were performed using the following conditions: 1.50 mL freshly prepared aqueous buffer solution ($[buffer]_{final}$ 5.00×10^{-2} M), buffer: MES (pH 4.00 to 6.50), HEPES (pH 7.00 to 8.50), CHES (pH 9.00 to 10.00) and CAPS (pH 10.50) with controlled ionic strength ($LiClO_4$) 0.10 M; 200 μL of an acetonitrile complex solution ($[C]_{final}=2.00\times10^{-5}$ M) and 300 μL of acetonitrile were added to a 1-cm-path-length cell. The reaction was initiated by the addition of 1.00 mL of an acetonitrile substrate solution ($[2,4\text{-bdnpp}]_{final}=2.50\times10^{-3}$ M) and monitored between 2 and 5% of reaction at 25 °C. The kinetic experiments under conditions of excess substrate were performed as follows: 1.5 mL of freshly prepared aqueous buffer CHES solution (at pH 9.00), $[buffer]_{final}= 5.00\times10^{-2}$ M, and 50 μL of an acetonitrile complex solution ($[C]final= 1.24\times10^{-5}$ M) were added to a 1-cm-path-length cell. The reaction was initiated with the addition of 2,4-bdnpp solution ($[2,4\text{-bdnpp}]_{final}=2.00\times10^{-4}$ to 6.80×10^{-3} M). Correction for the spontaneous hydrolysis of the 2,4-bdnpp was carried out by direct difference using a reference cell under identical conditions without adding the catalyst. The initial rate was obtained from the slope of the absorbance *vs*. time plot over the first 5 min of the reaction. The conversion of the reaction rate units was carried out using $\varepsilon=12{,}100$ M^{-1} cm^{-1} for 2,4-dnp and the initial concentration of the complex [31] . A kinetic treatment using the Michaelis–Menten equation approach was applied [1] . The deuterium isotopic effect on the hydrolytic process was evaluated following two reactions with identical conditions (*vide* experiments on the effect of pH) using CHES buffer (pH or pD 9.00, previously prepared), and a 100-fold excess of substrate in comparison to the complex concentration. The reactions were monitored at 400 nm and 25 °C.

*2.3 Synthesis of **HL** unsymmetrical ligand.*

The dinucleating ligand 2-[(4,7-diisopropyl-1,4,7-triazonan-1-yl)methyl]-4-methyl-6-{[(pyridin-2-ylmethyl)amino]methyl}phenol (**HL**) was synthesized by reductive amination [32] as follows.

In a 125 mL round-bottom flask 2.57 g (7.11 mmol; 361.53 g mol^{-1}) of $tacn^{i}pr_2mff$ [23] and 0.73 mL of 2-(aminomethyl)pyridine (0.77 g; 7.11 mmol; 108.14 g mol^{-1}; 1.05 g mL^{-1}) were mixed with 50 mL of methanol/THF (50% v/v) yielding a dark-yellowish solution which was stirred magnetically for 2 h. Imine reduction was initiated by adding small portions of $NaBH_4$ (0.27 g; 7.11 mmol; 37.82 g mol^{-1}) at room temperature where, after 1 h, the reaction turned a pale-yellow color. The pH was adjusted to 7 with HCl (2.0 M) and the solvent was evaporated under reduced pressure at 40 ^{o}C. To the remaining oil, 50 mL of dichloromethane were added and the mixture was washed twice with 30 mL of a saturated aqueous $NaHCO_3$ solution. The organic phase was dried over anhydrous Na_2SO_4 and the solvent was rotoevaporated under reduced pressure yielding a pale-yellow oil. Yield: 96 % (3.09 g, 6.82 mmol; 453.67 g mol^{-1}). Anal. Calc. for $C_{27}H_{43}N_5O$, FW = 453.66 g mol^{-1}: C, 71.48; H, 9.55; N, 15.44. Found: C, 71.57; H, 9.50; N, 15.50%. IR spectrum (KBr pellet, cm^{-1}): ν (O-H) 3431(*br*); ν ($C\text{-}H_{aliph}$) 2962-2817(s); ν_s (C=C) 1589 - 1478(*m*); δ_s ($C\text{-}H_{aliph}$) 1381(*s*); δ_{ass} ($C\text{-}H_{alif}$) 1381(*m*); δ (O-H) 1357(*m*); ν ($C\text{-}O_{phenol}$) 1246(*m*); ν_s (C-N) 1116(*m*); δ ($C\text{-}H_{ar}$) 755(*m*). ^{1}H-NMR (400 MHz, $CDCl_3$, δ, ppm): 0.96 (*d*, 12H, CH_3); 2.20 (*s*, 3H, CH_3); 2.51 (*s*, 4H, CH_2); 2.70 (*t*, 4H, CH_2); 2.88 (*hept*, 2H, CH_{iPr}); 2.98 (*s*, 4H, CH_2); 3.78 (*s*, 2H, CH_2); 3.84 (*s*, 2H, CH_2); 3.92 (*s*, 2H, CH_2); 6.73 (*s*, 1H, CH_{ar});

6.90 (*s*, 1H, CH_{ar}); 7.14 (*t*, 1H, CH_{ar}); 7.36 (*d*, 1H, CH_{ar}); 7.63 (*t*, 1H, CH_{ar}); 8.54 (*s*, 1H, CH_{ar}). The spectra are available in the supporting information file (Figures S2 and S3).

2.4 *Synthesis of* $[Ni^{II}Ni^{II}(L)(\mu\text{-}CH_3COO)_2(OH_2)]BPh_4 \bullet H_2O$ (***1***)

Complex **1** was synthesized through the dropwise addition of a **HL** ligand solution in acetonitrile (0.227 g; 0.5 mmol; 453.67 g mol^{-1}) to $Ni(ClO_4)_2 \cdot 6H_2O$ (0.366 g; 1.0 mmol; 365.69 g mol^{-1}) also dissolved in CH_3CN. The mixture was kept under magnetic stirring, at 40 ºC, for 30 min and 0.123 g (1.5 mmol; 82.03 g mol^{-1}) of CH_3COONa and 0.171 g (0.5 mmol; 342.22 g mol^{-1}) of $NaBPh_4$ were then added, resulting in a pale greenish solution. After a few minutes a green solid was formed. The crude complex was filtered and doubly recrystallized from acetonitrile to afford a green microcrystalline solid. Yield: 65% (0.339 g, 0.325 mmol) based on ligand. Anal. Calcd. for $C_{55}H_{72}BN_5Ni_2O_7$, FW = 1043.39 g mol^{-1}: C, 63.31; H, 6.96; N, 6.71. Found: C, 62.91; H, 5.57; N, 6.36%. IR spectrum (Kbr pellet, cm^{-1}): ν (O-H) 3440(*br*); ν (N-H) 3247(*s*); ν (C-H_{ar}) 3059-3034(*m*); ν (C-H_{aliph}) 2998-2851(*m*); ν (C=N and C=C) 1595(*s*) and 1472; ν (COO^-) 1422(*s*); ν (C-N) 1307(*w*), ν (C-O_{ph}) 1261(*w*); δ (C-H_{ar}) 735 - 707(*m*). Molar conductivity (CH_3CN, 1.0 mM) Λ_M = 108 μS.

3. Results and discussion

3.1. Synthesis and general characterization

The *N*-rich unsymmetrical **HL** ligand was synthesized in a one-pot reductive amination process through the addition of *2*-picolylamine to the

tacn^{i}Pr$_2$mff precursor (Figure S1, supporting information). The reaction was monitored through thin layer chromatography (TLC) and the product was characterized by IR and ^{1}H-NMR spectroscopy (see experimental section for further details).

Complex **1** was synthesized via the reaction of nickel(II) perchlorate and the ligand **HL** in a 2:1 stoichiometric ratio using acetonitrile as the solvent. The coordination reaction could be observed from the color change during the metal addition. Sodium acetate was added in order to neutralize the solution, deprotonate the **HL** ligand, and provide the μ-acetato bridging ligands. These features have been observed for several other complexes previously described in the literature [4] [6] [13] [15] [22] .

A variety of physical and chemical measurements were performed for **1**, both in the solid state and in the fluid solution. These methods include elemental analysis, molar conductivity, infrared and electronic spectroscopy, square-wave voltammetry and electrospray mass spectrometry. In order to demonstrate the acid/base properties of the complex, which allows an understanding of the phosphodiester catalytic cleavage, potentiometric titrations were also performed. Although much effort has been made to isolate single crystals of **1**, their fragility and poor quality prevent analysis using x-ray techniques.

3.2. Infrared spectroscopy and molar conductivity

Infrared spectroscopy was essential for the preliminary characterization of the ligand and its complex. A spectral overlay of the ligand **HL** and **1** is shown in Figure 1.

<< Please add Fig. 1 here, as a single-column picture >>

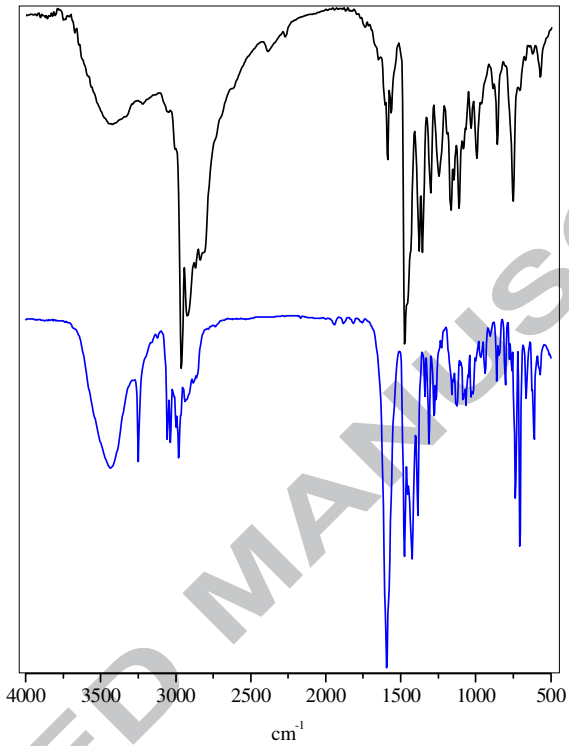

Figure 1. Overlay of the IR spectra for the **HL** (top) and **1** (bottom).

The infrared spectrum of **1** is mainly characterized by the skeletal ligand vibrations and the presence of exogenous species (bridging ligands) and the counterion. Despite the ligand deprotonation, the O-H stretching becomes more evident in **1** (3440 cm^{-1}), indicating the presence of water molecules bonded to a nickel center and acting as a crystallization solvent. This proposal was confirmed by the elemental analysis and ESI-MS. The spectrum for the complex reveals a sharp IR absorption peak at 3247 cm^{-1} attributed to N-H stretching, which is not resolved in the isolated ligand. This behavior could be associated with the ligand

rigidity after the complexation. The increase in the absorption at 1595 cm^{-1} in **1** strongly suggests the presence of the tetraphenylborate counterion, while the band broadening between 1472 and 1422 cm^{-1} indicates the presence of the bridging μ-OAc^- exogenous ligands. The intensity of the C-H out-of-plane angular deformation (δ_{CH}) at 755 cm^{-1} in **HL** also increased in **1**, as a second indication of the presence of the $B(Ph)_4^-$ counterion. A similar IR profile was observed by Greatti and co-workers [14] .

An acetonitrile solution of **1** was analyzed via molar conductometry [33] , where the cationic character of the complex was confirmed by the 1:1 electrolyte type (Λ_M = 108 μS). These data are in full agreement with the results of the elemental analysis, IR spectroscopy and electrospray mass spectrometry (*vide infra*).

3.3. Electrospray ionization-mass spectrometry

Electrospray ionization-mass spectrometry (ESI-MS) studies were performed on **1** in ultrapure CH_3CN (Figure 2) and both the positive and negative modes were monitored. For the positive scan mode six peak clusters were observed at mass to charge ratios (m/z) of 702.2, 686.2, 672.3 for monovalent species and 313.6, 306.6 and 299.6 for divalent species. The peak cluster assignments are shown in Table 1 and the isotopic distribution simulations are shown in Fig. S4.

<< Please add Fig. 2 here, as a single-column picture >>

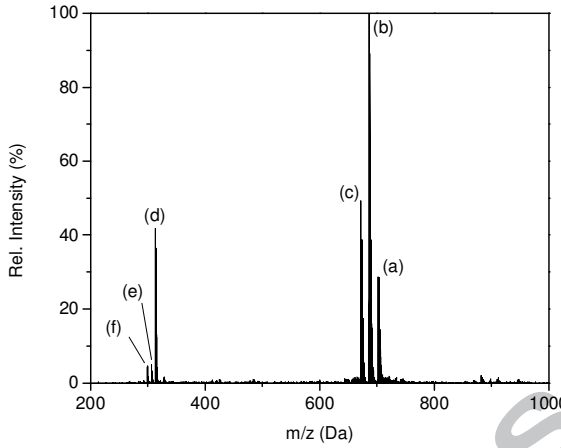

Figure 2. ESI-MS spectrum (positive mode) of **1** in acetonitrile.

The cluster at 702.2 Da (species "a", Table 1) is attributed to the cation complex $[Ni^{II}_2(L)(\mu\text{-}CH_3COO)_2(OH_2)]^+$, which confirms the obtainment of the structural unit aimed at for the cation complex during the synthetic procedure. The base peak cluster at 686.2 Da (100%) can be attributed to the loss of the aqua ligand in the softer nickel center, generating the moiety $[Ni^{II}_2(L)(\mu\text{-}CH_3COO)_2]^+$ (species "b", Table 1). Species "c" $[Ni^{II}_2(L)(\mu\text{-}OH)(CH_3CN)(CH_3CH_2OH)]^+$ at 672.3 Da is comprised of the ligand L and both the nickel centers bonded through a μ-hydroxo bridge. These data are in agreement with the results of the potentiometric titrations and kinetic studies (*vide infra*). Acetonitrile and ethanol molecules from the ion spray and acetate reduction, respectively, were also observed as exogenous ligands. This behavior has been previously described by Piovezan and co-workers [13] . The dicationic complex $[Ni^{II}_2(L)(\mu\text{-}CH_3COO)]^{2+}$, at 313.6 Da, (species "d", Table 1) is formed when "b" releases one of the intermetallic μ-acetato bridges into the ion spray. The cluster at 306.6 Da (species

"e", Table 1) is best interpreted as a dinuclear reduced Ni^{I}_2 species where the ligand is protonated (HL). The final mass fit is consistent with an ethanol molecule coordinated to a nickel center. The peak cluster with a lower relative intensity at 299.6 Da (species "f", Table 1) can be attributed to the $[Ni^{I}_2(HL)(CH_3OH)]^{2+}$ complex. This moiety is very similar to species "e" and is also generated in the ion spray during the experiment.

When **1** was scanned in the negative mode using the ESI-technique (Fig. S5) a single peak cluster was found at 319.2 Da (species "g", Table 1). The mass fit is in full agreement with the tetraphenylborate counterion, the presence of which was also confirmed by elemental analysis and infrared spectroscopy (1595 cm^{-1}).

<< Please add Table 1 here, as a single-column picture >>

Table 1. ESI-MS data for complex **1** in CH3CN.

m/z (Da)	Formula	Species
a = 702.2	$C_{31}H_{50}N_5Ni_2O_6$	$[Ni^{II}_2(L)(\mu\text{-}CH_3COO)_2(OH_2)]^{+}$
b = 686.1	$C_{31}H_{48}N_5Ni_2O_5$	$[Ni^{II}_2(L)(\mu\text{-}CH_3COO)_2]^{+}$
c = 672.3	$C_{31}H_{52}N_6Ni_2O_3$	$[Ni^{II}_2(L)(\mu\text{-}OH)(CH_3CN)(CH_3CH_2OH)]^{+}$
d = 313.6	$C_{29}H_{45}N_5Ni_2O_3$	$[Ni^{II}_2(L)(\mu\text{-}CH_3COO)]^{2+}$
e = 306.6	$C_{29}H_{47}N_5Ni_2O_2$	$[Ni^{I}_2(HL)(CH_3CH_2OH)]^{2+}$
f = 299.6	$C_{28}H_{45}N_5Ni_2O_2$	$[Ni^{I}_2(HL)(CH_3OH)]^{2+}$
g = 319.2	$C_{24}H_{20}B$	BPh_4^{-}

3.4. Electronic and redox properties

The electronic absorption spectrum for **1** recorded in acetonitrile solution is shown in Figure 3. As observed, all of the bands have low molar absorption coefficients, indicating ligand field (*d-d*) transitions, except that at 303 nm. In general, nickel(II) complexes in octahedral environments show three spin-allowed *d-d* transitions in the ranges 1250-900, 670-520, and 500-370 nm, with low molar absorptivity coefficients (< 30 mol L^{-1} cm^{-1}) [34]

Two broad absorption bands are observed at 621 nm (ε = 20 mol L^{-1} cm^{-1}) and 1005 nm (ε = 27 mol L^{-1} cm^{-1}), which can be assigned to the $^3A_{2g} \rightarrow {}^3T_{1g}$ (*F*) and $^3A_{2g} \rightarrow {}^3T_{1g}$ (*F*) transitions, respectively. A weak band is also observed at 790 nm (ε = 9 mol L^{-1} cm^{-1}), which is ascribed to the spin-forbidden transition $^3A_{2g} \rightarrow {}^1E_g$ (D). In addition to these transitions, another band is observed at 298 nm (ε = 3611 mol L^{-1} cm^{-1}), which can be attributed to a charge-transfer transition involving orbitals from nickel(II) and the pyridine ligand, as previously observed for other correlated complexes previously described in the literature [13] [15] [35] [36]

<< Please add Figure 3 here, as a single-column picture >>

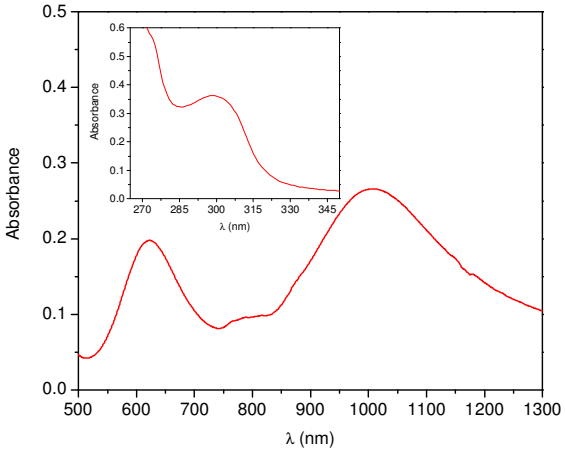

Figure 3. Electronic spectrum of complex **1** in acetonitrile solution (1.0×10^{-2} mol L^{-1}) and inset (1.0×10^{-4} mol L^{-1}).

The electrochemical behavior of **1** was determined by square-wave voltammetry in acetonitrile (0.1 mol L^{-1} *n*-Bu_4NPF_6 as supporting electrolyte). The best electrochemical response of **1** was obtained employing a gold working-electrode with a cathodic-direction scan. Table 2 shows the electrochemical data collected and the process attributions for **1** and other compounds described in the literature.

<< Please add Table 2 here, as a single-column picture >>

Table 2. Selected electrochemical data and process attributions for complex **1** and other complexes described in the literature.

Complex	Potential (V) *vs* NHE	Attribution	Ref.
1	-1.29	$Ni^{II/II} \rightarrow Ni^{II/I}$	This study
	-1.66	$Ni^{II/I} \rightarrow Ni^{I/I}$	
	1.00	$Ni^{II/II} \rightarrow Ni^{II/III}$	
	1.40	$Ni^{II/III} \rightarrow Ni^{III/III}$	
A	-1.27	$Ni^{II/II} \rightarrow Ni^{II/I}$	[13]
	-1.64	$Ni^{II/I} \rightarrow Ni^{I/I}$	
B	-1.41	$Ni^{II/II} \rightarrow Ni^{II/I}$	[37]
C	1.04	$Ni^{II/II} \rightarrow Ni^{II/III}$	[14]
	1.20	$Ni^{II/III} \rightarrow Ni^{III/III}$	

D	0.73	$Ni^{II/II} \rightarrow Ni^{II/III}$	[14]
	0.94	$Ni^{II/III} \rightarrow Ni^{III/III}$	

A = $[Ni^{II}_2(HBPPAMFF)(\mu\text{-}OBz)_2(OH_2)]BPh_4$; B = $[Fe^{III}Ni^{II}(bpbpmp)(\mu\text{-}OAc)_2]ClO_4$; C = $[Ni^{II}_2(L1)(\mu\text{-}CH_3COO)_2(OH_2)]ClO_4$; D = $[Ni^{II}_2(L2)(\mu\text{-}CH_3COO)_2(CH_3CN)]BPh_4$

The square-wave voltammogram (Fig. S6) reveals four irreversible electrochemical processes. Despite all efforts employed to improve the data acquisition, the cathodic waves (-1.29 V and -1.66 V versus NHE) are poorly resolved and the potentials can be attributed to the one-electron transfer processes $Ni^{II}Ni^{II} \rightarrow Ni^{II}Ni^{I} \rightarrow Ni^{I}Ni^{I}$, respectively. These data are indicative of the inability of the ligand to fully stabilize the $Ni^{II}Ni^{I}$ and $Ni^{I}Ni^{I}$ reduced species, although these values are in good agreement with the compound $[Ni^{II}_2(HBPPAMFF)(\mu\text{-}OBz)_2(OH_2)]BPh_4$ (**A**) previously described in the literature by Piovezan and coworkers [13] and similar to $[FeNi(bpbpmp)(\mu\text{-}OAc)_2]ClO_4$ (**B**) [37] .

The electrochemical response in the anodic region was found to be better than that in the cathodic region. Two waves were detected at 1.00 V and 1.40 V *versus* NHE and assigned to the irreversible stepwise one-electron oxidation couples $Ni^{II}Ni^{II} \rightarrow Ni^{II}Ni^{III} \rightarrow Ni^{III}Ni^{III}$. This redox behavior is also displayed by other dinuclear nickel(II) complexes described by Greatti and colaborators [14] .

Interestingly, the E_{ox1} ($Ni^{II}Ni^{II} \rightarrow Ni^{II}Ni^{III}$) for **1** (1.00 V) is comparable to that for compound **C –** $[Ni^{II}_2(L1)(\mu\text{-}CH_3COO)_2(OH_2)]^+$ (1.04 V versus NHE) where L1 is an unsymmetrical ligand containing three pyridine pendant arms [14] . This feature reveals that these nickel centers most probably have an equivalent O_4N_2-donnor set environment. When the E_{ox2} ($Ni^{II}Ni^{III} \rightarrow Ni^{III}Ni^{III}$) of **1** is compared with correlated compounds described by Greatti and coworkers a trend

can be observed: **D** (0.94 V) < **C** (1.20 V) < **1** (1.40 V). These results can be interpreted as reflecting the ability of the N_3O_3-coordination environment of each ligand to stabilize the oxidized species formed. In fact, better electron-density donors have lower oxidation potentials: **D** (pyridyl and *N*-methyl-imidazolyl groups), **C** (two pyridyl groups) and **1** ($^{i}Pr_2$-*tacn*).

3.5. Potentiometric titrations

In order to detect the presence of metal-bonded water molecules when complex **1** is in an aqueous solution, potentiometric titration experiments were carried out. This study can be carried out since the carboxylate-bridging ligands are labile in acetonitrile/water solutions [22] .

Experimentally, the titrations were performed in triplicate in a mixture of acetonitrile/water (50% v/v) with a constant ionic strength (0.1 M KCl), and they showed the neutralization of 3 mols of KOH per mol of complex in the pH range 2 to 12. Fitting the data with the BEST7 software [29] resulted in three discernible pK_a values: 5.14, 6.21 and 8.34. The corresponding species distribution diagram is shown in Figure 4, while the proposed deprotonation/protonation equilibrium steps can be seen in Chart 2.

<< Please add Figure 4 here, as a single-column picture >>

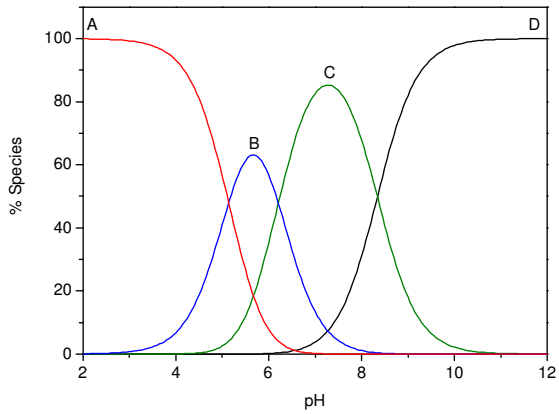

Figure 4. Species distribution curves of **1** as a function of pH. Experimental conditions: CH_3CN/H_2O 50% v/v, I = 0.1 mol L^{-1} (KCl).

The protonation equilibria can be interpreted in terms of the dissociation of the bridging-carboxylate groups (Chart 2) which in aqueous medium is in line with its well-documented lability, which is facilitated by increasing the pH of the solution [5] [22] .

Firstly, when **1** is dissolved in CH_3CN/H_2O at pH ~ 3.0 one acetate group is spontaneously released leading to the $\{(H_2O)Ni^{II}(\mu\text{-}OAc)Ni^{II}(OH_2)\}$ species (structure A) yielding one equivalent of acetic acid. The pK_{a1} (5.14) corresponds to the titration of this acid equivalent previously generated. After that, a release of the second carboxylate group to yield the $\{(H_2O)Ni^{II}Ni^{II}(OH_2)\}$ species occurs, where no exogenous bridging ligand is coordinated to the metal centers (structure B) and it reaches its maximum at pH 5.7 (63.1%). It has been proposed that upon the dissociation of the carboxylate groups, water molecules occupy the remaining coordination positions of the metal ions [5] [22] . It should be noted that the $\{Ni^{II}(\mu\text{-}OAc)Ni^{II}\}$ species with one carboxylate is present and no metal-bonded water molecules could be detected in the ESI-MS experiment (m/z = 313.6 Da,

Table 1). This feature could be interpreted as a lability parameter for water molecules and carboxylate anions bonded to the metal centers. Deprotonation of a metal-bonded water molecule generates the μ-OH bridge according to pK_{a2} = 6.21, yielding the species {$(H_2O)Ni^{II}(\mu\text{-}OH)Ni^{II}(OH_2)$} (structure C) with a maximum at pH 7.30 (85.3%). This pK_a value is in full agreement with similar dinuclear nickel(II) complexes described in the literature with compatible chemical environments [13] [14] . Once again, through the ESI-MS experiment, the μ-OH bridge could be found in solution at m/z = 672.3 Da, corresponding to the moiety $[Ni^{II}_2(L)(\mu\text{-}OH)(CH_3CN)(CH_3CH_2OH)]^+$. In the last step of the equilibrium process, pK_{a3} (8.34) is assigned to the deprotonation of the Ni^{II}-bound aqua ligand to yield structure D (Chart 2), which is predominant at pH values higher than 11.0 and in good agreement with published data on several complexes containing the Ni-OH_2 moiety [5] [13] [15] [22] [37]]. Indeed D is assigned as being the catalytically active species in the hydrolysis of diester bonds (*vide infra*).

<< Please add Chart 2 here, as a double-column picture >>

Chart 2. Proposed equilibrium of chemical species in CH_3CN/H_2O (50% v/v), for complex **1**.

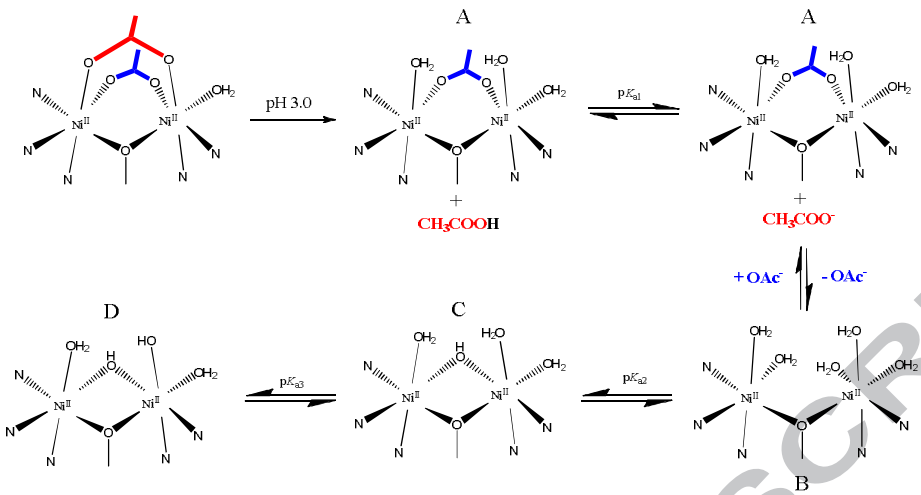

3.6. Phosphatase-like activity

The catalytic activity of complex **1** was evaluated in the hydrolysis reaction of the activated substrate 2,4-bdnpp [30] and monitored spectrophotometrically at 400 nm (ε = 12,100 $M^{-1}cm^{-1}$ of the 2,4-DNP^- anion) at 25°C, as described elsewhere [5] [22] The hydrolysis reaction was investigated in the pH range 4.00-10.5 and, as shown in Figure 5, the initial rates (v_0) versus pH plot for complex **1** has a sigmoidal shape. This curve was fitted by the Boltzmann model and a kinetic pK_a of 8.10 was obtained. This value is in good agreement with the pK_{a3} obtained from the potentiometric titrations (8.34) and with values reported for other dinuclear nickel(II) complexes in the literature (Table 3).

<< Please add Table 3 here, as a doubled-column picture >>

Table 3. pK_a values for the generation of selected species: {$(H_2O)M^{III/II}(\mu$-OH)Ni(OH_2)} (μ-OH exogenous bridge) and {$(H_2O)M^{III/II}(\mu$-OH)Ni(OH)} (terminal nucleophile) of complex **1** and other nickel(II) complexes described in the literature.

Species generated	**1**	**A**[13]	**B**[37]	**C**[14]	**D**[14]
	pK_a potentiometric/kinetic				
{$(H_2O)M^{III/II}$(μ-OH)Ni(OH_2)}	6.21/ -	6.19/ -	- / -	5.98/ -	6.65/ -
{$(H_2O)M^{III/II}$(μ-OH)Ni(OH)}	8.34/8.10	9.75/ -	8.61/ 8.30	9.70/9.20	8.20/7.80

A = $[Ni^{II}_2$(HBPPAMFF)(μ-OBz)$_2$(OH_2)]BPh_4; B = $[Fe^{III}Ni^{II}$(bpbpmp)(μ-OAc)$_2$]ClO_4; C = $[Ni^{II}_2$(L1)(μ-$CH_3COO)_2(OH_2)]ClO_4$; D = $[Ni^{II}_2$(L2)(μ-$CH_3COO)_2(CH_3CN)]BPh_4$

The agreement between the kinetic and the potentiometric pK_a values reinforces the proposal that deprotonation of a metal-coordinated water molecule is necessary to generate the catalytically active aqua-hydroxo {$(H_2O)Ni^{II}(\mu$-OH)Ni^{II}(OH)} species (*vide* Chart 2). Data obtained from these experiments also revealed that v_0 is highly influenced by alkaline pH, since for an increase in the pH from 4.0 to 8.0 the reaction rate increases by a factor of 135.

<< Please add Figure 5 here, as a single-column picture >>

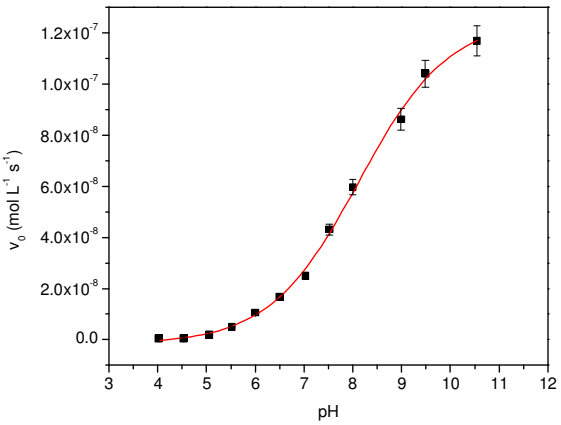

Figure 5. Dependence of the reaction rates (v_0) on the pH for **1** under the following conditions: H_2O/CH_3CN 50% solution, [complex] = 2.0×10^{-5} M, [2,4-BDNPP] = 2.5×10^{-3} M, [buffer] = 5.0×10^{-2} M (MES, HEPES, CHES, CAPS); I = 0.1 M ($LiClO_4$).

The effect of the diester 2,4-bdnpp concentration on the hydrolysis rate promoted by complex **1** was also investigated, and the experiments were carried out at pH 9.00 and 25 °C (Figure 6). As can be observed, the dependence of the initial reaction rate (v_0) on the 2,4-bdnpp concentration plots shows a linearity at low substrate concentrations and a saturation curve is obtained as the concentration increases, which suggest the formation of an intermediate complex-substrate. In view of this behavior, the data were treated using the Michaelis–Menten model and the kinetic parameters were obtained from a nonlinear least-squares fit. The complete kinetic data for **1** and similar compounds described in the literature by Piovezan [13] and Greatti [14] are listed in Table 4.

<< Please add Figure 6 here, as a single-column picture >>

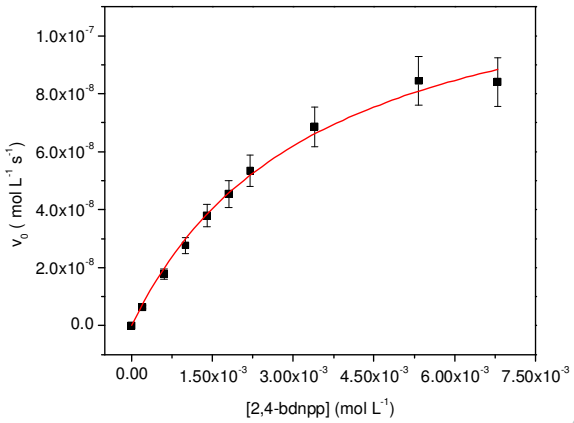

Figure 6. Dependence of the initial reaction rate (v_0) on the 2,4-bdnpp concentration for the hydrolysis reaction promoted by complex **1**. Conditions: [complex] = 1.24×10^{-5} mol L^{-1}; [buffer] = 5.0×10^{-3} mol L^{-1} (CHES, pH = 9.00); I = 5.0×10^{-2} mol L^{-1} ($LiClO_4$) in H_2O/CH_3CN (50% v/v) at 25 °C.

<< Please add Table 4 here, as a doubled-column picture >>

Table 4. Kinetic parameters for the 2,4-bdnpp hydrolysis promoted by **1** and other correlated dinickel(II) complexes described in the literature at pH 9.00 and 25 °C.

Complex	v_{max} (mol L^{-1} s^{-1}	K_M (mol L^{-1})	k_{cat} (s^{-1})	K_{assoc} (L mol^{-1})	E (L mol^{-1} s^{-1})	f
1	1.33×10^{-7}	3.44×10^{-3}	1.26×10^{-2}	291	3.70	3.25×10^{4}
A[13]	5.37×10^{-7}	1.57×10^{-3}	5.37×10^{-2}	637	34.2	13.8×10^{4}
C[14]	0.58×10^{-7}	1.19×10^{-3}	3.43×10^{-2}	840	28.8	8.83×10^{4}
D[14]	32.8×10^{-7}	5.67×10^{-3}	38.6×10^{-2}	176	68.1	99.5×10^{4}

A = $[Ni^{II}_2(HBPPAMFF)(\mu\text{-}OBz)_2(OH_2)]BPh_4$; B = $[Fe^{III}Ni^{II}(bpbpmp)(\mu\text{-}OAc)_2]ClO_4$; C = $[Ni^{II}_2(L1)(\mu\text{-}CH_3COO)_2(OH_2)]ClO_4$; D = $[Ni^{II}_2(L2)(\mu\text{-}CH_3COO)_2(CH_3CN)]BPh_4$. $K_{assoc} = 1/K_M$ (association constant); $E = k_{cat}/K_M$ (catalytic efficiency); $f = k_{cat}/k_{nc}$ (catalytic factor), where 3.88×10^{-7} s^{-1} at 25°C (uncatalyzed reaction constant) [30] .

The k_{cat} value calculated for **1** lies in the range of values found for complexes **A**, **C** and **D** previously reported for the same substrate [13] [14] However, **1** is 18 times less efficient (E/L mol^{-1} s^{-1}) than compound **D,** where the dinucleating ligand has two imidazolyl metal-donor groups attached. It should be noted that imidazole groups are present in proteins/enzymes in biological media. When these biomimetic groups are replaced with pyridines (dinucleating ligands for compounds **A** and **C**) the catalytic efficiency for both is approximately half that of **D**. Finally, during the synthesis of the ligand HL in this study two pyridines were substituted with the triazacyclonone macrocyclic ring, which explains the decrease in the *E* value, suggesting an influence from the ligand electron density imposed on the nickel centers by the *N*-donor aromatic rings.

In order to establish whether the nucleophilic attack on the phosphorus atom was via the terminal hydroxide ion or a general base catalysis, the isotopic effect was evaluated in the hydrolysis of 2,4-bdnpp in D_2O catalyzed by complex **1**. According to Burstyn and co-workers [38] , when $0.80 < (k_H/k_D) < 1.50$ this indicates that there is no proton transfer involved in the reaction limiting step, and suggests an intramolecular nucleophilic attack mechanism [39] . The k_H/k_D ratio obtained for **1** was close to 0.95, which corroborates the presence of a hydrolysis reaction proceeding through an intramolecular mechanism, in which the phosphorus atom undergoes a nucleophilic attack promoted by the coordinated hydroxide ion.

Conclusions and Outlook. – We synthesized a novel unsymmetrical dinucleating ligand containing a pyridine and *tacn*-derivative pendant arms via the route herein

described. This ligand seems to be suitable for obtaining the di-nickel(II) complex (**1**), as indicated by its physical and chemical properties observed through elemental analysis, molar electrical conductivity, IR and UV-visible spectroscopy, ESI-Mass spectrometry and electrochemistry. Potentiometric titrations confirmed the acid/base properties of **1** in acetonitrile/water solution. The {(HO)Ni^{II}(μ-OH)Ni^{II}(OH_2)} core is compatible with a catalytically-active species in the biomimetics previously reported in the literature. Complex **1** was able to catalyze the hydrolysis of the model substrate 2,4-bdnpp and, when compared with other similar complexes described in the literature, a trend could be noted, i.e., higher catalytic efficiency is observed for compounds which have aromatic *N*-donor moieties, such as imidazole and pyridine groups. Further studies with **1** on the catalytic cleavage of nucleic acids (DNA) to generate new potential drugs for technological applications, e.g., as anticancer agents, will be the subject of future reports.

Acknowledgement

The authors are grateful to CNPq, CAPES/Stint, INCT-Catálise, and FAPESC for financial support.

REFERENCES

[1] D.L. Nelson, M.M. Cox, Lehninger Principles of Biochemistry. 6th ed. (2012), New York: W. H. Freeman & Co, 1100 pp.

[2] G.K. Schroeder, C. Lad, P. Wyman, N.H. Williams, R. Wolfenden, Proc. Natl. Acad. Sci. U.S.A. 103 (2006) 4052.

[3] M.A. Zenkova, N.G. Beloglazova, in: M.A. Zenkova (Ed.), Nucleic Acids and Molecular Biology: Artificial Nucleases, vol. 13, Springer, Berlin, 2004.

[4] D.Desbouis, I.P. Troitsky, M.J. Belousoff, L. Spiccia, B. Graham, Coord. Chem. Rev. 256 (2012) 897.

[5] N.Mitic, S.J. Smith, A. Neves, L.W. Guddat, L.R. Gahan, G. Schenck, Chem. Rev. 106 (2006) 3338.

[6] A.L. Gavrilova, B. Bosnich, Chem. Rev. 104 (2004) 349.

[7] B.de Souza, R. Heying, A.J. Bortoluzzi, J.B. Domingos, A. Neves, J. Mol. Cat. A:Chem. 397 (2015) 76.

[8] V.R. Almeida, F.R. Xavier, R.E.H.M.B. Osório, L.M. Bessa, E.L. Schilling, T.G. Costa, T. Bortolotto, A. Cavalett, F.A.V. Castro, F. Vilhena, O.C. Alves, H. Terenzi, E.C.A. Eleuthério, M.D. Pereira, W. Haase, Z. Tomkowicz, B. Szpoganicz, A.J. Bortoluzzi, A. Neves, Dalton Trans. 42 (2013) 7059.

[9] R.E.H.M.B. Osório, R.A. Peralta, A.J. Bortoluzzi, V.R. de Almeida, B. Szpoganicz, F.L. Fischer, H. Terenzi, A.S. Mangrich, K.M. Mantovani, D.E.C. Ferreira, W.R. Rocha, W. Haase, Z. Tomkowicz, A. dos Anjos, A. Neves, Inorg. Chem. 51 (2012) 1569.

[10] N.A. Rey, A. Neves, A.J. Bortoluzzi, W. Haase, Z. Tomkowicz, Dalton Trans. 41 (2012) 7196.

[11] R.A. Peralta, A.J. Bortoluzzi, B. Szpogznicz, T.A.S. Brandão, E.E. Castellano, M.B. de Oliveira, P.C. Severino, H. Terenzi, A. Neves, J. Phys. Org. Chem. 23 (2010) 1000.

[12] N.A. Rey, A. Neves, P.P. Silva, F.C.S. Paula, J.N. Silveira, F.V. Botelho, L.Q. Vieira, C.T. Pich, H. Terenzi, E.C. Pereira-Maia, J. Inorg. Biochem. 103 (2009) 1323.

[13] C. Piovezan, J.M.R. Silva, A. Neves, A.J. Bortoluzzi, W. Haase, Z. Tomkowicz, E.E. Castellano, T.C.S. Hough, L.M. Rossi, Inorg. Chem. 51 (2012) 6104.

[14] A. Greatti, M. Scarpellini, R.A. Peralta, A. Casellato, A.J. Bortoluzzi, F.R. Xavier, R. Jovito, M.A. de Brito, B. Szpoganicz, Z. Tomkowicz, M. Rams, W. Haase, A. Neves, Inorg. Chem. 47 (2008) 1107.

[15] A. Greatti, M.A. de Brito, A.J. Bortoluzzi, A.S. Ceccato, J. Mol. Struct. 688 (2004) 185.

[16] T.P. Camargo, F.F. Maia, C. Chaves, B. de Souza, A.J. Bortoluzzi, N. Castilho, T. Bortolotto, H. Terenzi, E.E. Castellano, W. Haase, Z. Tomkowicz , R.A. Peralta, A. Neves, J. Inorg. Biochem. 146 (2015), 77.

[17] S.J. Smith, R.A. Peralta, R. Jovito, A. Horn, Jr., A.J. Bortoluzzi, C.J. Noble, G.R. Hanson, R. Stranger, V. Jayaratne, G. Cavigliasso, L.R. Gahan, G. Schenk, O.R. Nascimento, A. Cavalett, T. Bortolotto, G. Razzera, H. Terenzi, A. Neves, M.J. Riley, Inorg. Chem. 51 (2012) 2065.

[18] A. Neves, A.J. Bortoluzzi, R. Jovito, R.A. Peralta, B. de Souza, B. Szpoganicz, A.C. Joussef, H. Terenzi, P.C. Severino, F.L. Fischer, G. Schenk, M.J. Riley, S.J. Smith, L.R. Gahan, J. Braz. Chem. Soc. 21 (2010) 1201.

[19] A.C. Franzoi, R.A. Peralta, A. Neves, I. Cruz Vieira, Talanta 78 (2009) 221.

[20] A.J. Bortoluzzi, A. Neves, R.A.A. Couto, R.A. Peralta, Acta Cryst C62 (2006) m27.

[21] P. Karsten, A. Neves, A.J. Bortoluzzi, J. Strähle, C. Maichle-Mössmer, Inorg. Chem. Comm. 5 (2002) 434.

[22] L.R. Gahan, S.J. Smith, A. Neves, G. Schenk, Eur. J. Inorg. Chem. (2009) 2745.

[23] F.R. Xavier, A.J. Bortoluzzi, A. Neves, Chem. Biodivers. 9 (2012) 1794.

[24] J. Serrano-Plana, I. Garcia-Bosch. A. Company, M. Costas, Acc. Chem Res. 48 (2015) 2397.

[25] D. R. LIDE, 'Handbook of inorganic chemistry and physics', 81st ed., CRS Press, 2000. Section 5-91.

[26] M. Strohalm, M. Hassman, B. Košata, M. Kodíček, Rapid Commun. Mass Spectrom. 22 (2008) 905.

[27] M. Strohalm, D. Kavan, P. Novák, M. Volný, V.r. Havlíček, Anal. Chem. 82 (2010) 4648.

[28] R. Gagné, C. A. Koval, G. C. Lisensky, Inorg. Chem. 19 (1980) 2854.

[29] A.E. Martell, R. J. Motekaitis, 'Determination of Stability Constants', 2nd ed., VHC Publishers, Weinheim, Germany, 1992.

[30] C.A. Bunton, S.J. Farber, Journal of Organic Chemistry 34 (1969) 767.

[31] R.A. Peralta, A.J. Bortoluzzi, B. de Souza, R. Jovito, F.R. Xavier, R.A.A. Couto, A. Casellato, F. Nome, A. Dick, L.R. Gahan, G. Schenk, G.R. Hanson, F.C.S. de Paula, E.C. Pereira-Maia, S.P. Machado, P.C. Severino, C. Pich, T. Bortolotto, H. Terenzi, E.E. Castellano, A. Neves, M. J. Riley, Inorg. Chem. 49 (2010) 11421.

[32] I.A. Koval, D. Pursche, A.F. Stassen, P. Gamez, B. Krebs, J. Reedijk, Eur. J. Inorg. Chem. (2003) 1669.

[33] W.J. Geary, Coord. Chem. Rev. 7 (1971) 81.

[34] A.B.P. Lever, Inorganic Electronic Spectroscopy, 2nd ed.; Elsevier Science Publishers B.V.: Amsterdam, 1984; pp 553-572.

[35] S. Uozumi, H. Furutachi, M. Ohba, H. Okawa, D.E. Fenton, K. Shindo, S. Murata, D.J. Kitko, Inorg. Chem. 37 (1998) 6281.

[36] T.R. Holman, M.P. Hendrich, L. Que Jr. Inorg. Chem. 3 (1992) 937.

[37] G. Schenk, R.A. Peralta, S.C. Batista, A.J. Bortoluzzi, B. Szpoganicz, A.K. Dick, P. Herrald, G.R. Hanson, R.K. Szilagyi, M.J. Riley, L.R. Gahan, A. Neves, A. J. Biol. Inorg. Chem. 13 (2008) 139.

[38] J. N. Burstyn; K. A. Deal; A. C. Hengge. J. Am. Chem. Soc. 118 (1996) 1713.

[39] Gold, V. Advances in Physical Organic Chemistry; Academic Press: New York, 1967.

A novel unsymmetrical ligand HL and its dinuclear nickel(II) complex were synthesized. The ability to mimic the functional role of the dinuclear metalloenzymes was evaluated and the complex helped to probe the influence of the aromatic/aliphatic *N*-donor moieties, such as macrocyclic rings, pyridine and imidazole, through their catalytic efficiency parameter.